EasyChair Preprint

№ 2696

Investigation of Plastic Hinge Length for Reinforced Concrete Wall

Doaa Talib Hashim, Alyaa A. Al-Attar and Nabeel A. H. Kzar

February 18, 2020

Investigation of Plastic Hinge Length for Reinforced Concrete Wall

Doaa Talib Hashim [1], Alyaa A. Al-Attar[2], Nabeel A. H. Kzar[3]
{doaatalib7@gmail.com[1], dr.alyaa@ntu.edu.iq[2],
engineernabeel9@gmail.com[3]}

Mustansiriyah University, Baghdad, Iraq[1], Northen Technical University, Mosul, Iraq[2], Holy Karbala Municipalities, Hindiya Municipality, Karbala, Iraq[3]

Abstract. This study investigates the effect of certain parameters on the magnitude of plastic hinge length of RC shear walls and to propose an analytical expression for estimating the plastic hinge length. A finite element model was analyzed and validated with experimental test results for an existing study and a parametric study was performed for it. The established results were according to several parameters such as axial load ratio, slenderness ratio and wall length. The numerical results showed a different impact of these parameters on the formation of the plastic hinge length. In this study, a new simple expression was derived based on those parameters using statistical package software. Proposed plastic hinge expression was compared with the results of plastic hinge length obtained from FE analysis. Finally, the accuracy of the proposed equation was validated by using the shear wall results from literature researches.

Keywords: Plastic hinge length, Finite Element Analysis, Reinforced shear wall, Parametric study.

1 Introduction

Reinforced concrete (RC) shear walls are structural elements often used in buildings to provide lateral resistance and stiffness against earthquake and wind loads. These shear walls necessitate sufficient flexural displacement capacity and strength to have an acceptable seismic behavior.

The determination of amount and location of plastic deformations in RC shear wall considered a significant step for describing the performance of the shear wall building system in seismic loading. Although it was possible to consider that some ductility will be provided by beam hinges in structural systems, some rotational capacity of the reinforced concrete shear wall exists.

Many researchers have developed empirical models to investigate the parameters that affect the magnitude of plastic hinge region and to derive equations to calculate the length of plastic hinge in reinforced concrete elements depending on test results. These models are calibrated to obtain the total displacement at failure. Different parameters were considered in these models and each provides considerably different predictions. The influence of the member dimensions, the span length of the member and the longitudinal reinforcement properties were more considered by most of the previous researches. In addition, the influence of the axial load ratio and strain hardening were also studied. It is still unclear as to the most pertinent parameters that affect the plastic hinge length.

The plastic hinge length that is proportioned to the member's dimensions and axial load ratio was considered in many of these models. The shear wall dimensions have a large influence on deformations of slender shear walls that may be local or entire out of plane buckling especially for those that have low wall thickness. Moreover, out of plane buckling occurred at the base of the shear wall when high axial load applied to the shear walls.

The plastic hinge method and the derived analysis are still used widely in displacement-based seismic design and performance evaluation procedures for estimating the inelastic displacement demand and capacity [1].(Moehle, 1992) .

Although it was supposed that the inelastic curvature in the plastic region has a little variation, it is invariant along the plastic hinge length, Lp. The plastic curvature can be can calculated by the total curvature as shown in equation (1). Where Øy is yield curvature. By integrating the inelastic curvature, the inelastic rotation will be as shown in equation (2). Besides, by integrating the inelastic rotation, the inelastic displacement after considering the net height is shown in equation (3).

$$\emptyset p=\emptyset- \emptyset y \quad (1)$$

$$\theta p=\emptyset p\ Lp \quad (2)$$

$$L_n= L-\frac{L_p}{2} \quad (3)$$

$$\Delta_p=\theta_p\ L_n \quad (4)$$

$$\Delta_p=(\emptyset-\emptyset_y\ )\ L_p\ [L-\frac{L_p}{2}] \quad (5)$$

After combine equations 1 and 5 the total displacement is shown in equation (6). By integrating the elastic curvature, the yield displacement can be established. It was assumed that the elastic curvature linear (equation 7). As a result, the total displacement is as shown in euation (8)

$$\Delta_f=\Delta_y+\Delta_p=\Delta_y+(\emptyset-\emptyset_y\ )\ L_p\ [L-\frac{L_p}{2}] \quad (6)$$

$$\Delta y=\frac{\emptyset_y L^2}{3} \quad (7)$$

$$\Delta=(\frac{\emptyset_y L^2}{3}+(\emptyset-\emptyset_y)\ L_p\ [L-\frac{L_p}{2}] \quad (8)$$

By neglecting the shear deformation

$$\Delta=\Delta_f+\Delta_{sp} \quad (9)$$

$$\Delta_{sp}=\frac{2}{3}\ \emptyset_e\ \ L_{sp}\ h_w \quad (10)$$

$$L_{sp}= 0.15\ f_y\ d_{bl} \qquad (11)$$

The shear deformation in slender concrete walls was estimated using the experiential equation was developed [2]. This experiential equation was formulate based on a series of experimental and analytical studies of slender RC walls under seismic loading as shown in the following eqution (12) and (13).

$$\Delta_{sh}=1.5\ \Delta_f\ [\frac{\varepsilon_m}{\emptyset \tan\beta}]\ \frac{1}{h_w} \qquad (12)$$

$$\Delta_u=\Delta_f+\Delta_{sp}+\Delta_{sh}=(\frac{1}{3}\ \emptyset e\ h_w^2+\frac{2}{3}\ \emptyset e\ L_{sp}\ h_w+\emptyset_p\ L_p\ h_w\ )(1+1.5(\frac{\varepsilon_m}{\emptyset \tan\beta}))\ \frac{1}{h_w}) \qquad (13)$$

Traditional plastic hinge analysis is depended on the theory of an elasto-plastic behavior and an equivalent length of plastic hinge. The yield curvature used in equation (5) can be determined considering that the moment-curvature relationship in the plastic hinge zone is elasto-plastic [3]. This approximation depended on the actual shape of the moment-curvature relationship. **Figure 1** shows the equivalent yield curvature for a shear wall.

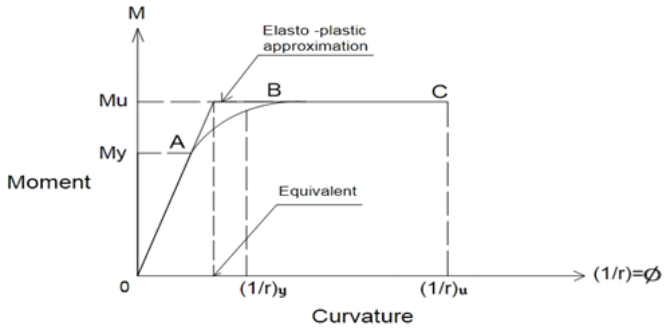

Fig. 1. Schematic moment-curvature curve for the cross section of an elasto-plastic material according to the approximation [3].

Many of studied investigated the effect of the member depth on the plastic hinge length. They found that it has a significant impact on the length of plastic hinge. Besides, [4] investigated the plastic distortions of hinges in concrete frames. He showed that a safe estimation of the plastic hinge length in columns was between 0.5h and h. Where, h: is the depth of column. Through the progress report on code clauses for "Limit Design" [5], suggested lower and upper bounds for the plastic hinge length in beams and frames.

In addition, it was suggested an expression to calculate the plastic hinge length for RC components [6]. Equivalent length of plastic-hinge can be assumed to be as one-half the element depth. Where L_w is the wall length. Moreover, it has been proposed equivalent plastic hinge that can set to be at 0.2 times the wall length, L_w, plus 0.07 times the moment-to-shear ratio (M/V) (equation 14) [7].

$$L_p=0.2\ L_w+0.07(M/V) \qquad (14)$$

Besides, it has been proposed an expression to calculate the plastic hinge length in Eurocode 8 as shown in equation (15). Where: Lv = shear span (moment-shear ratio, M/V), d_{bl} = (mean) diameter of the tension reinforcement, fy and f'c are yield stress of the longitudinal reinforcement and compressive strength of the concrete, respectively [8].

$$L_P = \frac{L_v}{30} + 0.2L_w + \frac{d_{bl}\, f_y(MPa)}{\sqrt{f'_c(MPa)}} \qquad (15)$$

In addition, [9] conducted tests on reinforced concrete members subjected to uniaxial bending, with and without axial loads, to derive expressions for plastic hinge length and deformations at yielding and failure, in terms of the member geometric and mechanical properties. They developed equations (15) and (16) to calculate the length of plastic hinge:

For cyclic loading:

$$L_{p,cy}= 0.12L_S+ 0.014\ \alpha_{sl}\ f_y\ d_b \qquad (16)$$

For monotonic loading:

$$L_{p,mon}=1.5L_{p,cy}=0.18L_S+ 0.021\ \alpha_{sl}\ f_y\ d_b \qquad (17)$$

$L_{p,cy}$: Plastic hinge length for cyclic loading, $L_{p,mon}$: Plastic hinge length for monotonic loading, α_{sl}:Zero-one variable (it is equal to one if slippage of the longitudinal reinforcement is possible, and zero if it is not possible), fy: Yield stress of the tension reinforcement, in MPa units.

Moreover, models have been developed for beams, rectangular columns or walls and members of T-, H-, U- or hollow rectangular section, with or without detailing for earthquake resistance and with continuous longitudinal bars [10]. They employed a databank of cyclic or monotonic tests to flexure-controlled failure to develop/calibrate models for the curvature and the chord rotation of reinforced concrete members at flexure-controlled ultimate conditions – at a 20% post-ultimate strength drop in lateral force resistance – under monotonic or cyclic loading. They proposed expressions to calculate the length of plastic hinge for both cyclic and monotonic loading (equations 18 and 19):

$$L_{pl,cy} = 0.2\,h\left[(1+\tfrac{1}{3}min\left(9;\tfrac{L_s}{h}\right)\right] \quad \text{For cycling loading} \qquad (18)$$

$$L_{pl,mon} = h\left[(1.1+0.04\,min\left(9;\tfrac{L_s}{h}\right)\right] \quad \text{For monotonic loading} \qquad (19)$$

Where h is the depth of the member, Ls is the shear span.

Conducted finite element analysis model validated by test results on RC structural wall [11]. They proposed an expression depend on the results of nonlinear finite element analysis, an expression for Lp as a function of wall length, moment-shear ratio, and axial compression equation (20)

$$L_p = \frac{\Delta_{pf}}{\emptyset_p L} = 0.5L_{pr} + L_{sp} \qquad (20)$$

Where P = axial force on the section, and Aw = wall area. They concluded that there was a complex interaction between walls with different Lw. A parametric study was presented to determine the length of plastic hinge of circular RC columns using a three-dimensional finite element analysis [12]. They examined some parameters included the longitudinal reinforcing ratio, the shear span-to-depth ratio, the axial load ratio and the concrete compressive strength. They proposed simplified formulas for the plastic hinge length of circular reinforced concrete columns equations (21) and (22).

$$\frac{L_p}{h} = 0.936\left(\frac{P}{P_o}\right) + 7.398\left(\frac{A_s}{A_g}\right) + 0.06\left(\frac{L}{h}\right) - 0.003\left(f'_c\right) \quad \text{For 414 MPa} \qquad (21)$$

$$\frac{L_p}{h} = 0.503\left(\frac{P}{P_o}\right) + 3.218\left(\frac{A_s}{A_g}\right) + 0.053\left(\frac{L}{h}\right) - 0.0018\left(f'_c\right) \quad \text{For} \quad 685 \text{ MPa} \qquad (22)$$

(As/Ag) Longitudinal reinforcing ratio, (L/h) Shear span-to-depth ratio, P/Po Axial load ratio. They made a comparison between the three dimensional finite element model and experimental results. Good agreement has been seen for the comparison that been made. Besides, A parametric study was conducted to derive an analytical expression for estimating the length of plastic hinge for cantilever RC structural walls by using the results of comprehensive nonlinear finite-element analyses [13]. It was showed that variation of plastic zone length at the base of the cantilever wall depends on several parameters, such as the wall length, wall height, axial load ratio, and the ratio of wall boundary element and the web horizontal reinforcement. In this parametric investigation, a plastic hinge length expression was proposed dependent on wall length, axial load ratio, wall horizontal web reinforcement ratio, and shear-span-to-wall-length ratio equation (23).

$$L_p = 0.27L_w\left(1 - \frac{\mathrm{P}}{A_w f'_c}\right)\left(1 - \frac{\mathrm{fy}\rho_{sh}}{f'_c}\right)\left(\frac{\mathrm{M/V}}{L_w}\right)^{0.45} \qquad (23)$$

P = axial force on the section, and fy and fc=yield stress of the longitudinal reinforcement and compressive strength of the concrete, respectively, M/V= shear span , Lw = wall length and ρsh=horizontal reinforcement of web section. The accuracy and reliability of the proposed plastic hinge length equation was verified using the available shear wall test results. Moreover, it was conducted a parametric study on the curvature distribution over the member length of RC shear wall using a non-linear, two-dimensional, finite-element analysis procedure to propose a simple model that can determine the potential plastic hinge region for seismic design [14]. It was done on the basis of Bernoulli's principle, strain compatibility condition an equilibrium condition of forces. They simply formulated the plastic hinge length of the shear wall as a function of longitudinal tensile reinforcement index in the boundary element, vertical shear reinforcement index in the web, and axial force index. The predicted length of plastic hinge is shown in equation (24).

$$l_p = h_w\left(1 - 0.91\Lambda^{0.1} + \zeta_{shear}\right) \qquad (24)$$

$$\Lambda = \omega_s + \omega_v^{1.3} + \omega_p^{1.4} \qquad (25)$$

$$\zeta_{shear} = 0 \ \ for\ V_n \leq V_c \qquad (26)$$

$$\zeta_{shear} = 0.38\,\Lambda^{-0.15}\left(\frac{l_w}{h_w}\right) for\ V_n > V_c \qquad (27)$$

They concluded that the predicted plastic hinge length that was obtained from the present simple model was in better agreement with test results than for the previous equations in that the mean, standard deviation and coefficient of variation of the ratios between experiments and predictions are 1.019, 0.102 and 0.100, respectively.

For these reasons, finite element analysis was conducted using ABAQUS software on several models to investigate the parameters which have a significant effect on plastic deformation in plastic zone. Also, this analysis is to obtain an equation for plastic hinge length of slender walls. Several models will be created by including some parameters that decrease or prevent out of plane buckling failure and to get an equation for plastic hinge length of slender walls using ABAQUS finite element software. Before doing these models, a calibration model of a cantilever shear wall [2] was considered to generate key parameters in the model and then analyzed on experimental test results for a specified specimen that are taken from previous tests. The geometrical, material, and loading values are adapted from experimental specimens reported in the literature, and the experimental results are then used to validate the computational models. This will be done to know how well the finite element results for model accurate match the test results.

2 Finite Element Analysis

A concrete reinforced shear wall was modelled using finite element method. It is common practice to use finite elements in simulating behavior of structural members. ABAQUS (v6.14) was selected to carry out this study. Half-scale experiment results [2] that were available from a previous research were used as the reference and compared with the ABAQUS analysis results. Finite element analysis and model of cantilever shear wall was developed and set as the initial control for the investigation purpose of this project work. The work by (Dazio et al., 2009) [2] was used as the reference for comparison with result from the finite element analysis .Therefore, all the parameters and conditions in the laboratory test were used in the modelling process. The parameters are given in the following subsections.

2.1 Control Specimen

The control specimen was prepared as shown in Fig. 1 and Fig. 2 .The size and the dimensional details of the cantilever RC shear wall have been used according to lab experiment conducted by (Dazio et al., 2009) [2] of quasi-static cyclic tests and plastic hinge analysis of RC structural walls. It consists of two main parts as following:
The first part which was a cantilever shear wall of 5.55m height, 2m width and 0.15 m thick. It has a thicker portion located at the top of the shear wall than the thickness of other shear wall part. The details of reinforcements are comprised of (34 longitudinal bars, 22 rebars with Ø 8 diameter and 12 rebars Ø 12 diameter) and (horizontal rebars with two straight bars Ø 6 @ 150 mm and U shape bars Ø 6 @ 150 mm) .Some properties are shown in Table 1, 2, and 3.

Table 1. Summary of the test unit properties [2].

Test unit	Sectional forces at the base	Reinforcement ratios	Stabilizing reinforcement

	N (kN)	$N/A_g f'_c$(_)	$V/0.8 l_w b_w$	$\alpha_N = 0.45 l_w \frac{N}{M}$(	ρ_{bound} (%)	ρ_{web} (%)	ρ_{tot} (%)	ρ_h (%)	s (m)	$\frac{s}{D_{nom}}$(_)
WSH4	695(+/-)6	0.057	1.85	0.31	1.54	0.54	0.82	0.25	No ties	

Table 2. The reinforcing steel properties for control specimen (WSH4) [2].

D_{nom} (mm)	$R_{p02}(MPa)$	$R_m(MPa)$	$\frac{R_m}{R_{p02}}$(_)	A_{gt}	classification $\frac{R_m}{R_{p02}} - A_{gt}$	Class(_)
12(6x)	576.0 ± 2.6	674.9 $\pm$ 1:8	1.17 ± 0.01	7.29 ± 0.61	H _ M	B (~C)
8(6x)	583.7 ± 5:5	714.4 ± 5.1	1.22 ± 0.01	7.85± 0.66	H _ H	C
6 (6x)	518.9 ± 13:8	558.7 ± 6:7	1.08 ± 0.02	5.45 ± 0.41	M _ M	B

Table 3. Mechanical properties [2].

Test unit	ρ_c(kg/m³)	f_{cw} (MPa)	f'_c (MPa)	E_c (GPa)
WSH4	2378 ± 15	58.8 ± 1.7	40.9 ± 1.8	38.5 ± 2.0

The second part is beam foundation that was supporting the upper shear wall. It consisted of a beam fixed boundary condition with 2.8m height, 0.7m width and 0.6 m height. The details of reinforcements are comprised of (8 rectangular shaped bars $\emptyset$ 18 diameter and U shaped 28 rebars with $\emptyset$ 12 diameter) (**Figure 2**).

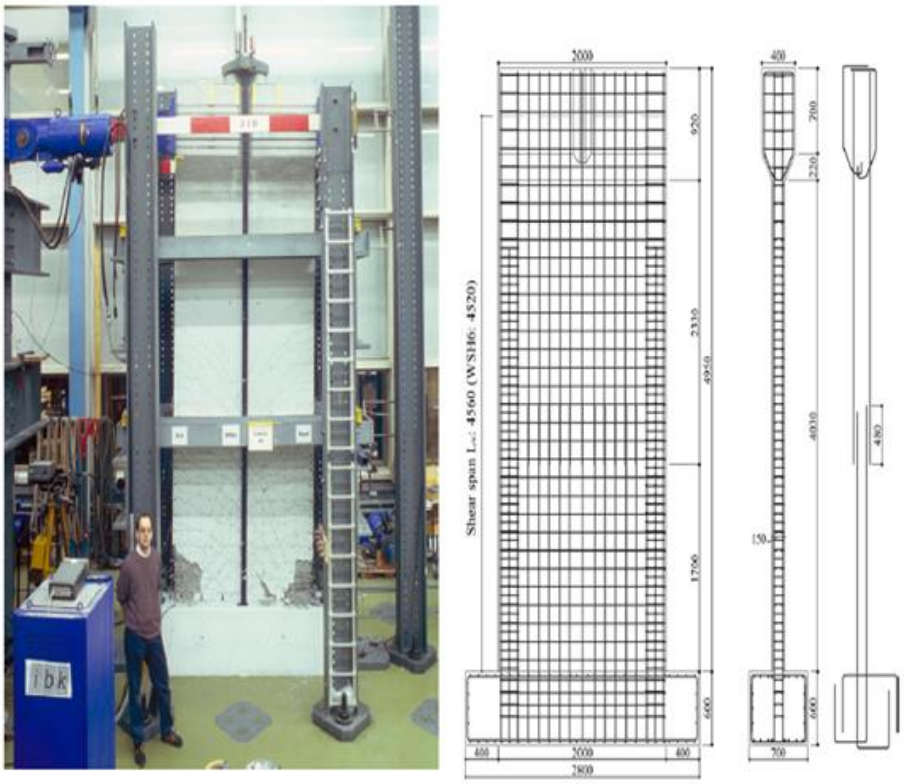

Fig. 2. Experimental Framework and Specimen Dimensions (Dazio et al., 2009).

2.2 Structural Modelling in ABAQUS

2.2.1 Modelling Shear walls

Nine models were geometrical modelled as well as a model of control specimen to validate FEA results with test results. Dimensional (3D) and deformable solid of type extrusion were used to create parts as shown below in **Figures 3 and 4**.

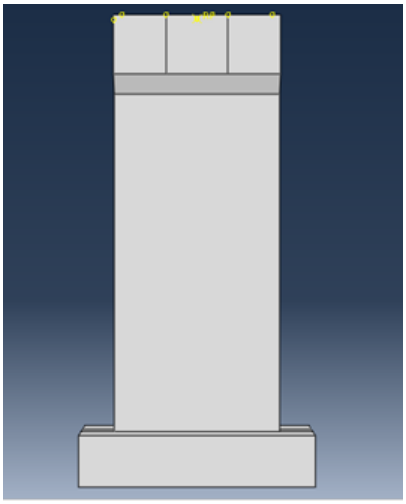

Fig. 3. Shear wall module.

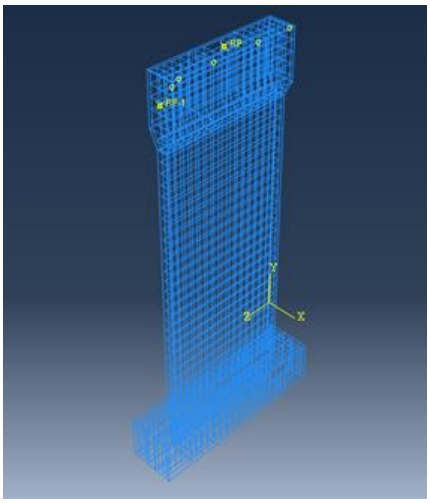

Fig. 4. Shear wall reinforcement.

2.2.2 Creation of Parametric Models

New finite element models of RC shear wall were created with different parameters that are as following:

1. Three models with varying thickness to wall height ratio (tw⁄Hw) 0.02 for (t = 10 cm) , 0.024 for (t = 12cm) and 0.028 for (t = 14 cm)), other dimensions and properties will remain the same for the three models. These three models labeled as following:
   Model (M1) with the thickness to wall height ratio of (tw⁄Hw) (0.02) (t=10 cm)).
   Model (M2) with the thickness to wall height ratio (tw⁄Hw) (0.024) (t = 12 cm)).
   Model (M3) with the thickness to wall height ratio (tw⁄Hw) (0.028) (t = 14cm)).

2 Three models with varying wall length ((Lw = 1.75 m), (Lw = 1.5 m) , (Lw = 1.25 m)), other dimensions and properties will remain the same. These three models labeled as following:
Model 4 (M4) with wall length (Lw) (Lw = 1.75 m).
Model 5 (M5) with wall length (Lw) (Lw = 1.5 m).
Model 6 (M6) with wall length (Lw) (Lw = 1.25 m).

3 Three models with varying axial load ratio 0.075 for (P= 925 kN), 0.1 for (P = 1230 kN), and 0.2 for (P = 1840 kN), other dimensions and properties will remain the same. These three models labeled as following:
Model 7 (M7) with axial load ratio 0.075 (P= 925 Kn).
Model 8 (M8) with axial load ratio 0.1 (P= 1230 Kn).
Model 9 (M9) with axial load ratio 0.15 (P = 1840 Kn).

The cantilever shear wall and beam foundation were modeled by eight-node solid elements with a reduced-integration scheme (C3D8R) (**Figure 5a**). Two node truss elements were modeled the steel reinforcement using (T3D2) (**Figure 5b**). The size of the mesh of the whole model was chosen based on the required accuracy. The truss elements were embedded in and fully bonded to the solid elements (**Figure 5c**).

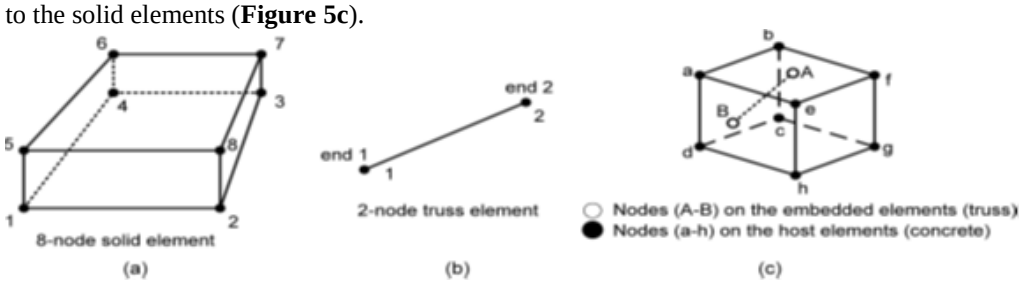

Fig. 5. (a) 8-node element (C3D8R), (b) truss element (T3D2) and (c) embedded constraint.

All modelled parts were assembled together in such a way that they can mimic the experimental study according to the mentioned details. Besides, the maximum element size of the mesh was 100 mm as shown in **Figure 6**.

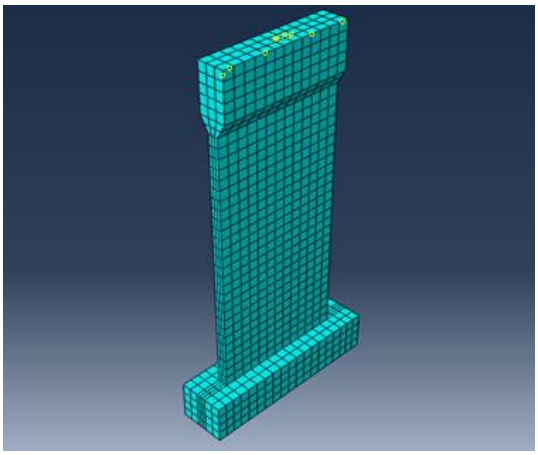

Fig. 6. Mesh of the ABAQUS Model.

2.2.3 Material Models

The properties of the materials were used to be the same for the real model in the experimental test for precise simulation through a computational effort. Therefore, the material models are required in this study to characterize the inelastic behavior of concrete and steel. The Mander's model was established by Mander et al., 1988 to simulate the behavior of concrete that was chosen as the analytical model (**Figure 7**) and (**Figure 8**). Mander's model has been verified analytically and experimentally. This constitutive model was based on the Popovics equation [15]. The tensile stress-strain behavior of concrete was assumed to behave like the compression model with the peak stress and strains equal to 10% of the its values. The analytical model for concrete in compression is described in equation (28)

$$f_c = \frac{f'_{cc}\, xr}{r-1+x'} \quad (28)$$

f_c : confined compressive strength (MPa)

f'_{cc} : Compressive strength of confined concrete

$$x = \frac{\varepsilon_c}{\varepsilon_{cc}} \quad (29)$$

ε_c : Longitudinal compressive concrete strain

$$\varepsilon_{cc} = \varepsilon_{co}\left[1 + 5\left(\frac{f'_{cc}}{f'_{co}} - 1\right)\right] \quad (30)$$

$$r = \frac{E_c}{E_c - E_{sec}} \quad (31)$$

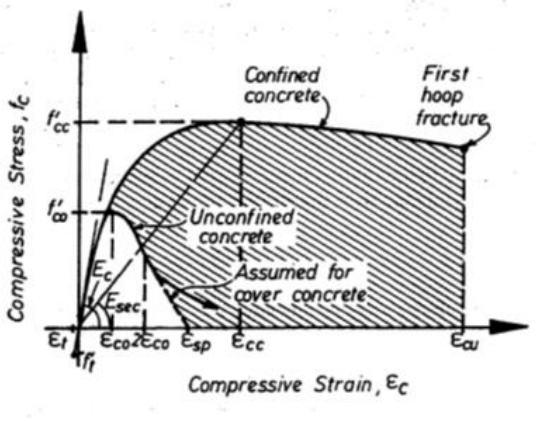

Fig. 7. Stress - strain behavior for confined and unconfined concrete for monotonic loading [16].

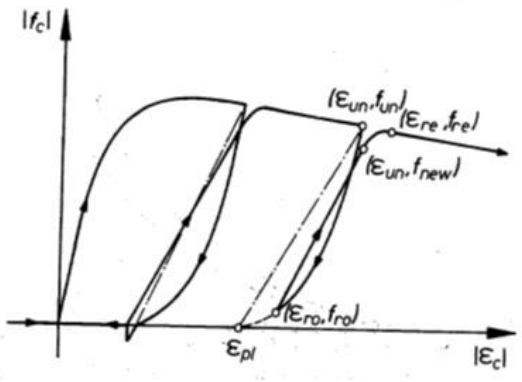

Fig. 8. Stress - strain behavior for confined and unconfined concrete for cyclic loading [17].

2.2.3.1 Concrete Damaged Plasticity Model

The assumption of scalar (isotropic) damage depended by the concrete damaged plasticity model and the applications used concrete that is subjected to arbitrary loading conditions, including cyclic loading. The degradation of the elastic stiffness induced by plastic straining both in tension and compression is taken into consideration. It also accounts for stiffness recovery effects under cyclic loading. The concrete damaged plasticity model is based on the plasticity model supposed by Lubliner et al., 1989 [18] and Lee et al., 1998 [19].The salient features of model are discussed here.

2.2.4 Loads and Boundary Conditions

2.2.4.1 Boundary Conditions for models

In ABAQUS software, the boundary conditions for all models have been created to derive an equation to calculate the plastic hinge length with fixed support at base and roller support at the base of shear wall. This is to make the base of the shear wall fixed and to prevent the vertical movement at the top of shear walls that may lead mistakes in results.

2.2.4.2 Load Cases

An axial load which was chosen to be the same for six models of shear walls and variables with respect to other three models. Axial load assigned to be constant throughout the analysis process that will be applied on the top surface of the model with magnitude of 695000 N according to the experimental test [2] as shown in **Figure 9**.

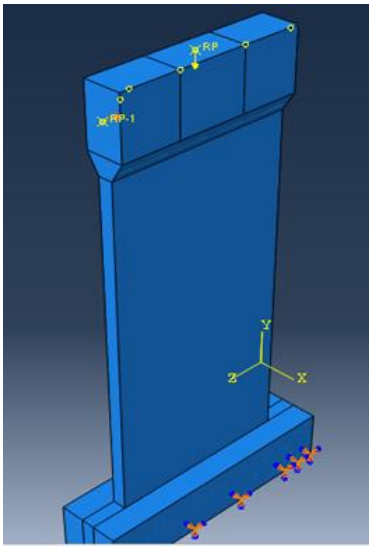

Fig. 9. Applied concentrated axial load.

Besides, a quasi-static monotonic load that was taken from the experimental test [2] has been applied on the model. The horizontal cyclic displacement history consisted of two cycles at each ductility level was applied to the wall's head which (**Figure 10**). The first two cycles were force controlled while the following ones were displacement-controlled. In the first two cycles the wall was loaded until the force equaled 3/4 of the nominal yield force F_y. The nominal yield displacement Δ_y was then determined as 4/3 times the average peak displacement reached during these first cycles. A small loading velocity was chosen to keep dynamic effects to a minimum and to allow a continuous control of the instrumentation and the hydraulic system. For larger amplitude cycles the loading velocity was gradually increased. Moreover, a monotonic load was applied in order to establish many results relevant to curvatures and rotation which can be obtained by applying cyclic loading as shown in **Figure 11**. A nonlinear analysis was adopted to predict the components of yield and ultimate curvature under monotonic and axial loads.

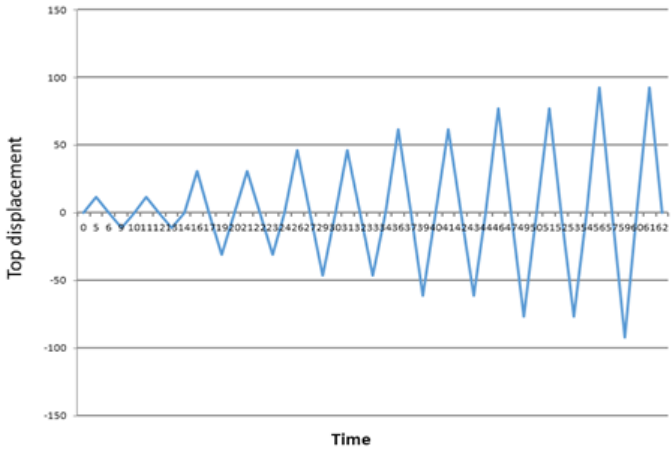

Fig. 10. Load History [2].

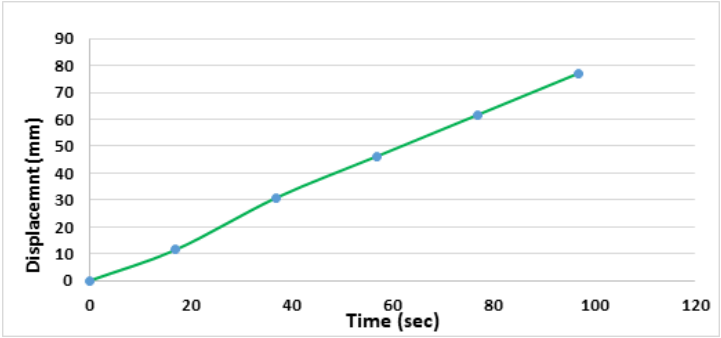

Fig. 11. Monotonic Loading.

3. Determination of Plastic Hinge Length (L_p)

Plastic hinge length was determined according to equation (32) that was derived from plastic hinge section analysis for the cantilever shear wall as stated in the introduction.

$$\Delta_f = \frac{\emptyset_y L^2}{3} + (\emptyset - \emptyset_y) L_p \left[L - \frac{Lp}{2}\right] \quad (32)$$

When steel and concrete strains for each element at the same row are obtained, the ultimate curvature was calculated according to Kazaz, 2013 [13] as following.

$$\emptyset_b = \frac{\varepsilon_s - \varepsilon_c}{L} \quad (33)$$

Then, the moment- curvature curve was plotted for whole models. The maximum lateral force that was applied to the RC shear wall was corresponding to a maximum drift of (δ=1.36 %) as stated in Dazio et al., 2009. This drift ratio considered as a damage limit state for other models. The ultimate curvature was limited to the base section at the first element.

3.1 Derivation of Plastic Hinge Length Equation

The multiple regression technique was adopted in deriving the expression by SPSS statistics software. Multiple regression allows the simultaneous testing and modeling of multiple independent variables. There were 9 results of parametric models and 3 results of reference mode that were equal 12 results as stated in Table 4. Plastic hinge length calculated as a function of the following parameters: (a) slenderness ratio (t_w/H_w) axial load ratio ($\frac{P}{A_w f_c'}$) and wall length (L_W). Plastic hinge length results were input as a dependent variable while the identified parameters were considered as independent variables which are as following:

Table 4. The parameters input as independent variables into SPSS software.

($\frac{P}{A_w f_c'}$)	(t_w/H_w)	(L_W)(mm)
0 .058	0.03	2000
0.075	0.03	2000
0.1	0.03	2000
0.15	0.03	2000
0.058	0.03	2000
0.058	0.02	2000
0.058	0.024	2000
0.058	0.028	2000
0.058	0.03	2000
0.058	0.03	1750
0.058	0.03	1500
0.058	0.03	1250

The nonlinear analysis was adopted because there are more than one parameter and this type of analysis is realistic and comprehensive to get more accurate and reliable equations. The correlation (square R) was calculated in SPSS software for each trial. At first, each parameter will be individually checked whether which one of them acts linearly or not.

3.1.1 Validation of proposed plastic hinge length expression

First, the proposed expression was verified with the previous plastic hinge length equations that derived numerically by checking its correlation to others individually. In order to validate the accuracy of the analytically derived plastic hinge length expression, a database composed of shear wall test results was collected. The database is composed of 24 small-to-large-scale shear wall tests; 15 specimens were tested under static cyclic loading of either increasing or variable displacement amplitude. The significant properties and a summary of primary experimental results are presented in Table 5. Standard deviation and convergence were calculated in the correlation curve plotted.

Table 5. Differences between experimental and FE results.

Ave. of Finite Element Results	Ave. of Experimental Work Results	Average displacement difference %	Average force

Force (Kn)	Disp. (mm)	Force (Kn)	Disp. (mm)		difference %
0	0	0	0	0	0
379.27	11.28	308.787	11.27	0.062	18.58
403.5	30.52	421.6	30.89	1.2	4.5
375.225	45.725	429.775	46.37	1.39	14.53
364.42	60.23	426.5	61.7	2.38	17.03
366.13	77	331.2	77.1	0.13	9.54

4. Results of the Parametric Study

4.1 Loads vs Displacements

As shown in the graphs plotted below that related load-displacement curves are for nine parametric models that has been analyzed. It has been shown in **Figure 12** for M1, M2 and M3 that when the axial load ratio ($P/f_c'A_w$) increased, the capacity of maximum load was also significantly increased at the same horizontal displacements. Therefore, this increment has led to increase the ultimate moments for FE models. However, maximum drift ratios reduced as they were increased.

It could be seen in **Figure 13** for M4, M5 and M6 when thickness to wall length ratios (t_w/H_w) were slightly increased, the ultimate load capacities were also increased, thus these increment led to increase the drift ratio for models. As obvious from **Figure 13** the resistant load was not highly dropped after it was reached yielding displacement as compared with (1),(2) and (3) models. This indicates that this parameter has a good effect on optimizing the load capacity which was not highly sensitive to very small changes of this parameter because out of plane buckling failure was largely affected by changing thicknesses of RC shear walls subjected to both of axial and lateral loads. It can be seen in **Figure 14** that when the wall lengths were decreased, the load and moment capacity have reduced. Moreover, it can be noted that the deference between these curves was highly big because of the inherent correlation between moment capacities and wall lengths therefore load capacities increase by increasing wall lengths.

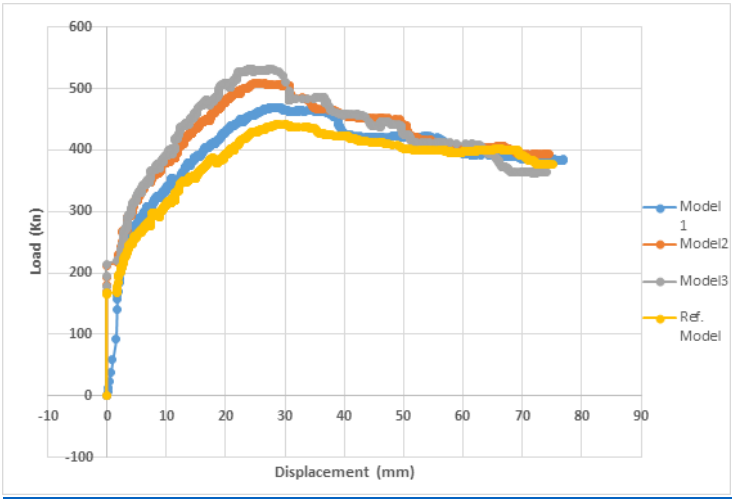

Fig. 12. Load vs Displacement for models (1), (2) and (3).

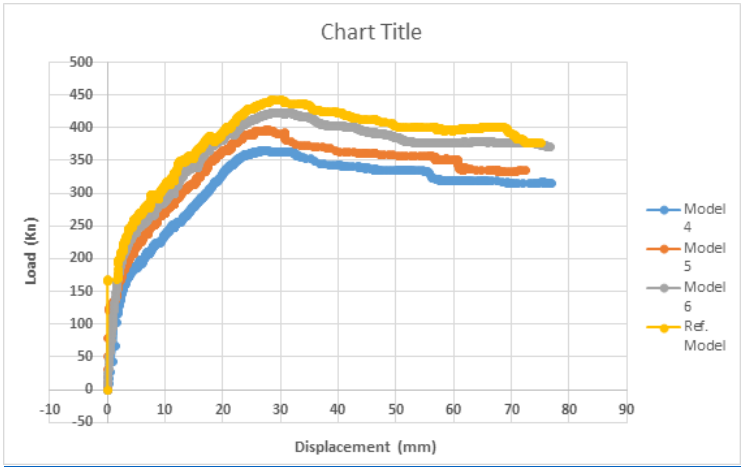

Fig. 13. Load vs Displacement for models (4), (5) and (6).

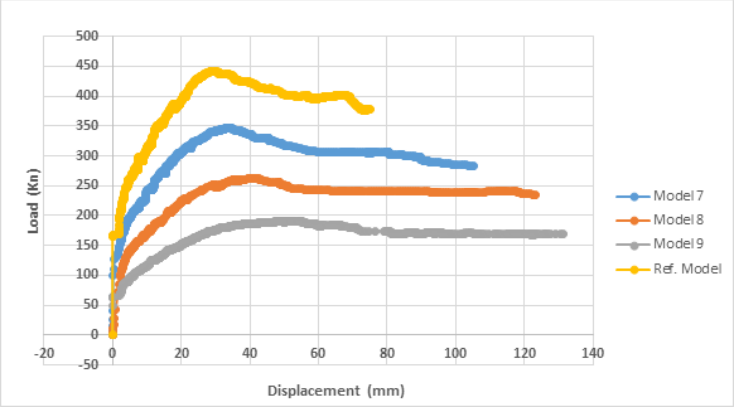

Fig. 14. Load vs Displacement for models (7), (8) and (9).

4.2 Moment - Curvature Curves for Parametric Models

Moment – Curvature curve shown in **Figure 15** has stated that base section curvatures for models (1), (2) and (3) were considerably affected by the parameter of axial load ratio when it decreased they increased. This took place when drift ratios were less than that determined for the reference model due to early failure damage of the unconfined concrete in the compression zone. Drift ratios at which base section curvatures were calculated for these models were of $\delta(1.16\%,\ 1.04\%\ and\ 0.865\%)$ respectively. This also decreased the tensile strains of reinforcing bars in tension zone of models and thus the total base section curvatures had been reduced. As shown in **Figure 16**, base section curvatures for models (4), (5) and (6) have been slightly changed when thickness to wall length ratios were small varied because of the little effect of this parameter on base curvatures. Drift ratios at which base curvatures were determined for these models were of $\delta(1.18\%,\ 1.24\%\ and\ 1.33\%)$. Due to unconfined concrete or no stabilizing reinforcement in compression, out of plane buckling could be highly affected by reducing this parameter. In **Figure 17** as noted, reducing wall lengths for models (7), (8) and (9) led to increase the base section curvatures. Due to a big reduction of wall length models, crushing compression zone regions were limited to a small area at the wall bases. Thus, drift ratios at which base curvatures were determined for these models considerably increased that were of $\delta(1.88\%\ ,\ 2.4\%\ and\ 2.66\%)$. Therefore, this parameter had a significant effect in increasing base curvatures and drift ratios.

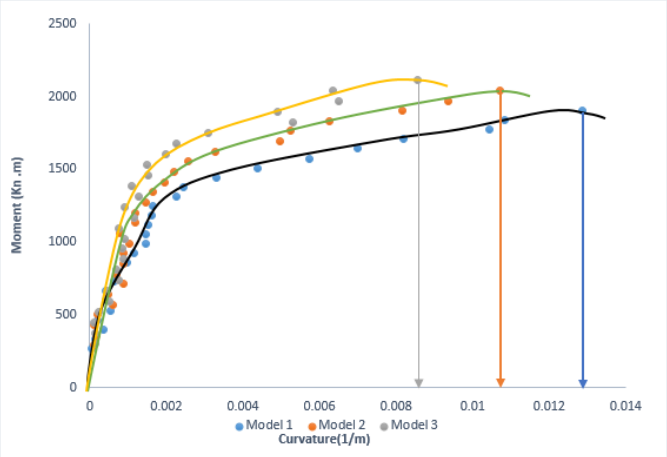

Fig. 15. Moment – Curvature Curve for models (1), (2) and (3).

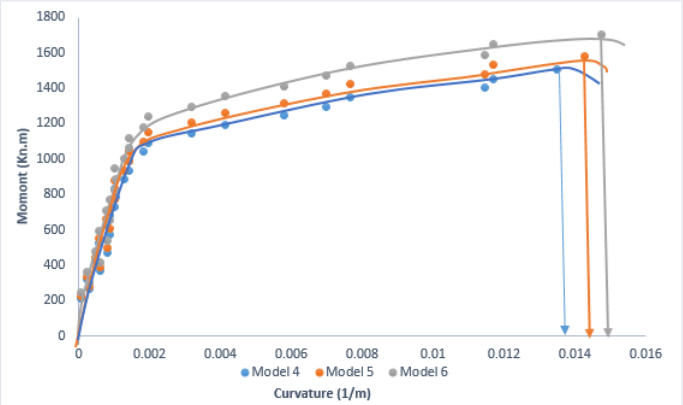

Fig. 16. Moment – Curvature Curve for models (4), (5) and (6).

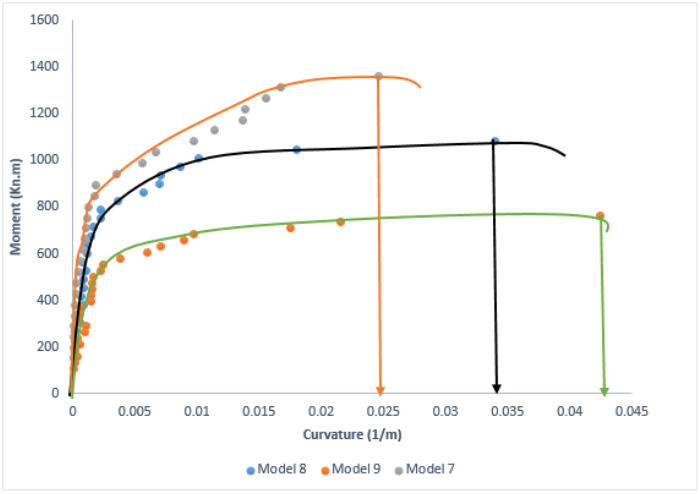

Fig. 17. Moment – Curvature Curve for models (7), (8) and (9).

4.3 Plastic Hinge Lengths for Parametric Models

As explained in section 3, the plastic hinge lengths could be done by both two ways but the best fit line as shown in **Figures 18** and **19** considered more accurately than the direct way by applying the equation 32.

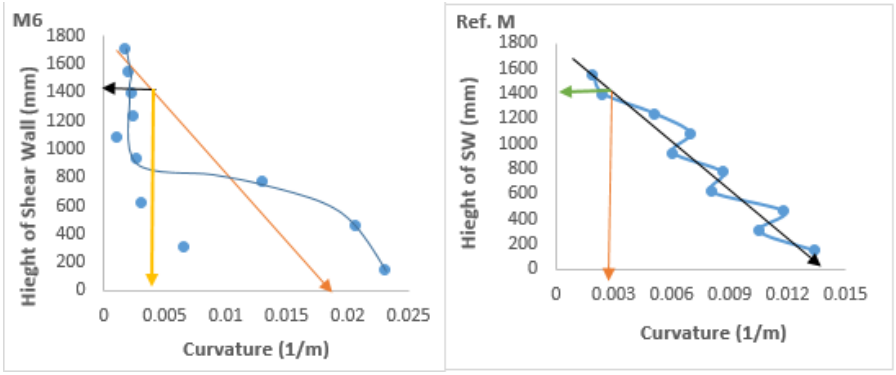

Fig. 18. Calculation of plastic hinge zone for reference and model (6).

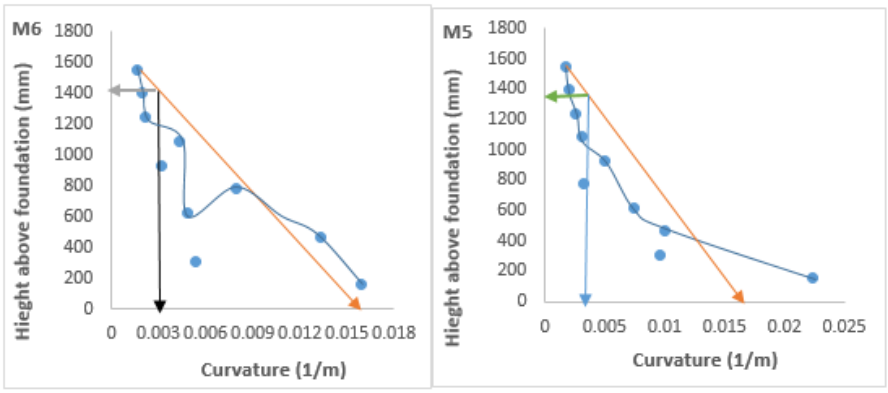

Fig. 19. Calculation of plastic hinge zone for model (4) and model (5).

According to plastic hinge length results presented in Table 6, it can be noted that the most one of the parameters that has apparently significant effect on the plastic hinge length is the wall length of models. In fact, the ratio of thickness to wall height is the most parameter has a considerable impact on the results of plastic hinge length especially when the wall thickness is bigger more than 10mm. Since the out of plane buckling failure may be frequently occurred in RC shear wall for which thicknesses are less than 10 mm, increasing thickness of RC walls within this range can be useless for purposes of the plastic hinge length calculations. Moreover, the RC shear wall model found to have no confining or stabilizing reinforcement, therefore total out of plane buckling or reinforcing bars at the compression zone to be buckled may be often occurred even when wall thicknesses more than 10 mm. Thus, this could adversely influence on generating plastic hinge lengths and so on the ductility demands.

Table 6. Plastic hinge length results and the corresponding parameters.

Symbol of model	$L_P(mm)$	R_{AL}	R_{Ht}	L_w(mm)
MR	724	0.058	0.03	2000
M1	701	0.075	0.03	2000
M2	682	0.1	0.03	2000
M3	638	0.15	0.03	2000
M4	681	0.058	0.02	2000
M5	698	0.058	0.024	2000
M6	716	0.058	0.028	2000
M7	656	0.058	0.03	1750
M8	606	0.058	0.03	1500
M9	552	0.058	0.03	1250

4.3.1 Axial Load Ratio Parameter

As shown in **Figure 20** plastic hinge lengths for reference (1), (2) and (3) have increased as the parameter of axial load ratios decreased. In contrary, lengths of plastic hinge decreased as base

section curvature increased as stated in **Figure 21**. Consequently, this parameter has inverse proportion with the plastic hinge length and direct proportion with the base curvature.

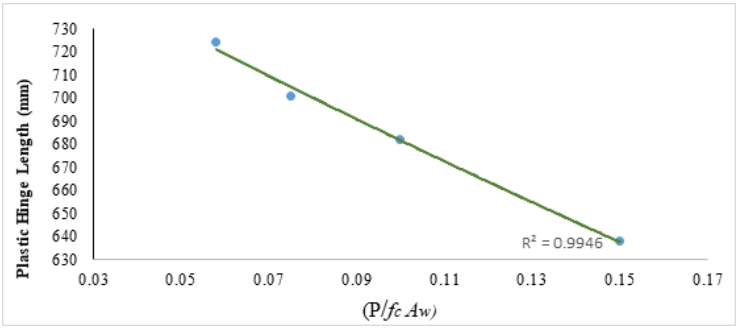

Fig. 20. Plastic Hinge Length Vs Axial Load Ratio parameter for reference, (1), (2) and (3) models.

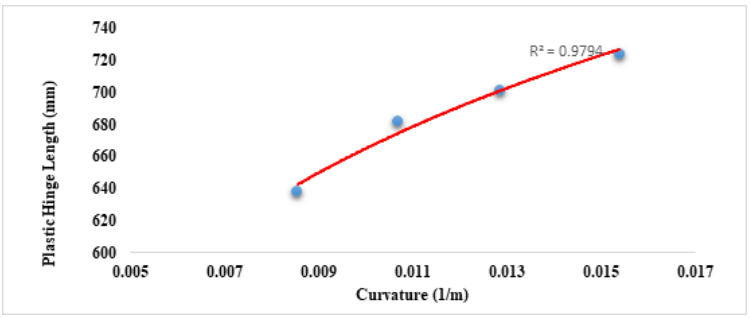

Fig. 21. Plastic Hinge Length Vs Curvatures of axial load ratio parameter for reference, (1), (2) and (3) models.

4.3.2 Thickness to Wall Height Ratio Parameter

As shown in **Figure 22** plastic hinge lengths for reference (4), (5) and (6) had increased when the parameter of thickness to wall height decreased. In contrary, lengths of plastic hinge increased as base section curvature increased as stated in **Figure 23**. Consequently, this parameter has inverse proportion with the plastic hinge length and direct proportion with the base curvature.

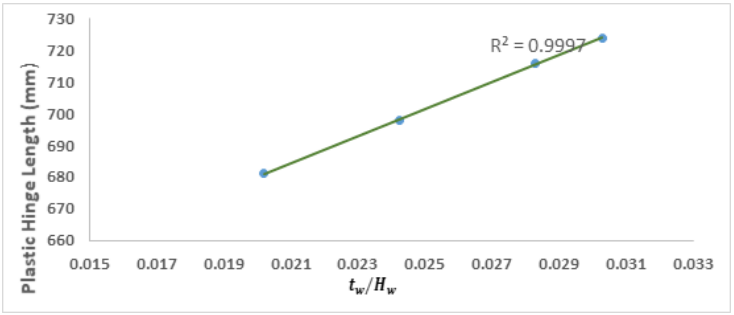

Fig. 22. Plastic Hinge Length Vs Thickness to Wall Height Ratio parameter for reference, (4), (5) and (6) models.

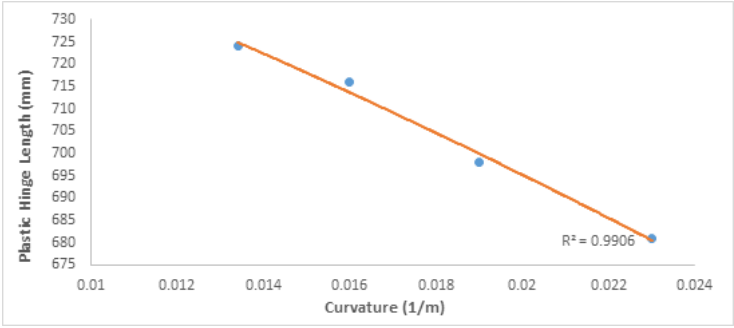

Fig. 23. Plastic Hinge Length Vs Curvatures of Thickness to Wall Height ratio parameter for reference, (4), (5) and (6) models.

4.3.3 Wall Length Parameter

As shown in **Figure 24** plastic hinge lengths for reference (4), (5) and (6) had increased when the parameter of the wall length increased. Consequently, this parameter has direct proportion with the plastic hinge length and the inverse proportion with base curvature.

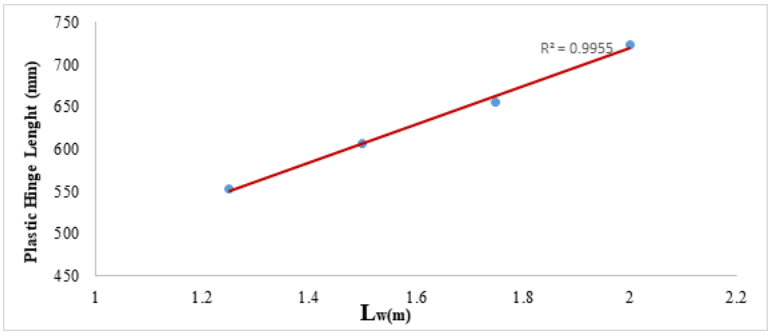

Fig. 24. Plastic Hinge Length vs Wall Length parameter for reference, (7), (8) and (9) models.

6. Derived Plastic Hinge Length Equation

As seen in **Figures 18**, **20**, and **22** all terms of the required equation checked to know how sensitive its correlation on the value of the plastic hinge length. It is found that the relationship between both axial load ratio and wall length parameters and the plastic zone length weas linear whereas the relation between the thickness to wall height ratio was nonlinear. Based on these findings, the analytical equation was derived as shown in equation (34).

$$L_p = (0.293\, L_w)\,(1 - 1.38\,\frac{P}{f_c' A_w})\ *(\ \frac{1}{0.033*(R_{ht}/L_w)^{-0.28}}\ ) \qquad (34)$$

As seen in **Figure 25a**, the proposed expression derived in this study has good agreement and correlation when compared with the plastic hinge length obtained from FE analysis results. As shown in the output file of SPSS software, the R squared related to the accuracy of the derived equation was 92.6%. It can be concluded that the terms of the proposed equation were linear except for the third term that was nonlinear. The plastic hinge length prediction using the derived equation (34) and available from other studies also was compared with finite element analysis

results in **Figures 25b**, **26**, and **27**. It is seen in these figures that the best predictions and correlations were obtained by equation (34) proposed in this work.

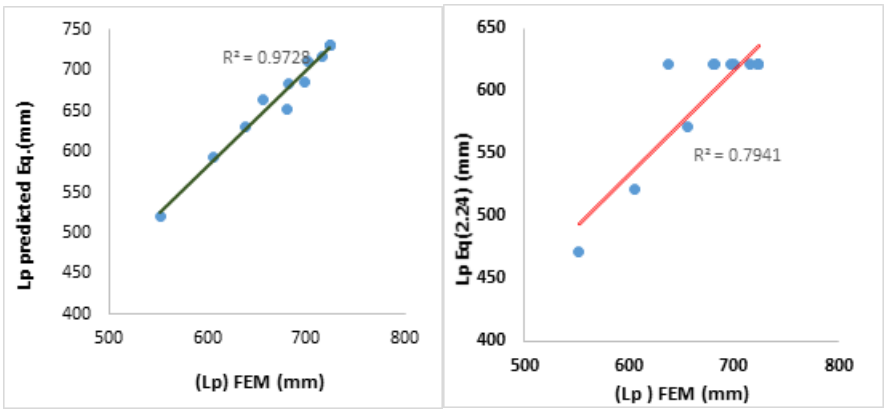

Fig. 25. Comparison of plastic hinge length calculate from FE analysis with predicted equation proposed in (a) this study, Eq. (34); (b) Eurocode 8.

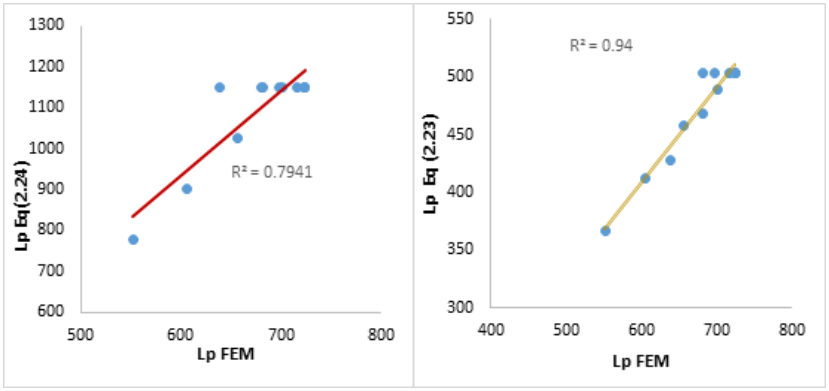

Fig. 26. Comparison of plastic hinge length calculate from FE analysis with (a) Priestley et al. (1996) [20]; (b) According to [7].

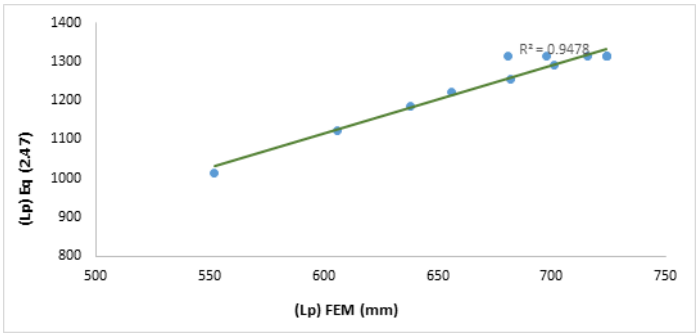

Fig. 27. Comparison of plastic hinge lengths calculated from finite-element analysis with the Bohl and Adebar (2011) [11].

6.1 Verification of proposed expression using experimental data

Validating the accuracy of the (L_p) expression that derived analytically, a database comprised of shear wall test results was compiled. The data composed of 23 small-to-large-scale shear wall experiments was tested under static cyclic or monotonic loading of either increasing or variable displacement amplitude. The significant properties and a summary of test results are presented in Table 7. It was noted that although there are several experimental tests on RC shear walls, a few of them only organized the plastic zone length L_{pz} data. The calculated plastic hinge lengths for the predicted equation equation (34) are tabulated in the last column of Table 7 as the plastic zone lengths via multiplying them by 2. A comparison between the experimental and calculated L_{pz} values is shown in **Figure 28**. Standard deviation, covariance and the correlation degree were displayed as statistical information between the experimental and predicted values of L_{pz}. It was noted when compared between two last columns of from Table 7 and Figure 28, that there was a clear difference between measured and predicted values. That happened because the predicted results of the plastic zone length were calculated only based on three parameters as explained previously. In addition, all data presented in the Table 7 in columns (3), (4), (5) and (6) that concern parameters of the proposed equation did not provide a wide variety of data. Experimental values of the plastic zone length determined on the basis of many variables presented in the others columns contributed significantly to the calculation of L_{pz} . These were the reasons that made high standard deviation, a little covariance and a weak correlation between the experimental and predicted values.

Table 7. Test Parameters and Measured Deformations at Yield and Ultimate Displacement of Wall Specimens [13].

No. of specimen	specimen	L_w (cm)	t_w(cm)	H_w (cm	ρ_b %	ρ_{sv} %	ρ_{sh} %	R_{al} %	f_c' Mpa	$\frac{V_{ma}}{A_w\sqrt{f}}$	DR %	L_{pz} (exp.)	L_{pz} Pred.
1	PCA-R1	191	10.2	457	1.47	0.25	0.31	0.4	44.7	0.09	2.26	1.83	1.403
2	PCA-R2	191	10.2	457	4	0.25	0.31	0.4	46.4	0.16	2.92	2.06	1.403
3	PCA-B1	191	10.2	457	1.11	0.29	0.31	0.3	53	0.19	2.89	2.06	1.403
4	PCA-B2	191	10.2	457	3.67	0.29	0.63	0.3	53.6	0.49	2.27	1.83	1.403
5	PCA-B3	191	10.2	457	1.11	0.29	0.31	0.3	47.3	0.21	3.93	2.13	1.403
6	PCA-B4	191	10.2	457	1.11	0.29	0.31	0.3	45	0.25	5.94	2.74	1.403
7	PCA-B5	191	10.2	457	3.67	0.29	0.63	0.3	45.3	0.58	2.77	1.83	1.403
8	PCA-B6	191	10.2	457	3.67	0.29	0.63	14.1	21.8	0.9	1.71	1.52	1.136
9	PCA-B7	191	10.2	457	3.67	0.29	0.63	7.9	49.3	0.71	2.89	2.29	1.26
10	PCA-B8	191	10.2	457	3.67	0.29	1.38	9.3	42	0.77	2.86	2.29	1.23

11	PCA-B9	191	10.2	457	3.67	0.29	0.63	8.9	44.1	0.75	3.02	2.29	1.24
12	PCA-B10	191	10.2	457	1.97	0.29	0.63	8.6	45.6	0.53	2.77	2.13	1.243
13	PCA-F1	191	10.2	457	3.89	0.3	0.71	0.4	38.5	0.69	1.11	1.83	1.402
14	UCB-SW3	239	10.2	309	3.52	0.83	0.83	7.8	34.8	0.76	5.67	2	1.65
15	UCB-SW4	239	10.2	309	3.52	0.83	0.83	7.5	35.9	0.69	2.25	2	1.66
16	UCB-SW5	241	10.2	309	6.34	0.63	0.63	7.3	33.4	0.64	2.24	1.8	1.673
17	UCB-SW6	241	10.2	309	6.34	0.63	0.63	7	34.5	0.6	2.33	1.4	1.68
18	UCB-RW2	122	10.2	382	2.89	0.33	0.33	7	43.7	0.25	2.19	0.9	0.97
19	WS2	200	15	452	1.32	0.3	0.25	5.7	40.5	0.19	1.39	1.4	1.5
20	WS3	200	15	452	1.54	0.54	0.25	5.8	39.2	0.24	2.04	1.7	1.5
21	WS4	200	15	452	0.67	0.27	0.25	12.8	38.3	0.24	1.37	1.4	1.34
22	WS6	200	15	452	1.54	0.54	0.25	10.8	45.6	0.29	2.07	1.6	1.386
23	WI	163	12.7	1133	0.66	0.45	0.45	10	35	0.11	2	1.9	0.9

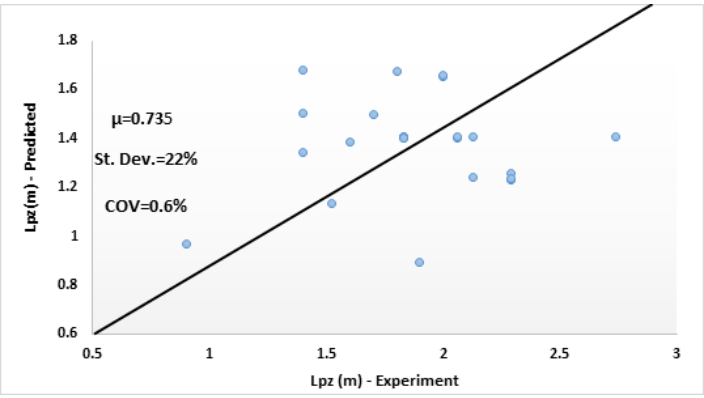

Fig. 28. Comparison of plastic zone lengths between measured and predicted.

7. Conclusion

The findings of this numerical study are summarized in the following:

1. Comparison of the FE analysis results to the experimental results displayed good agreement in the load–displacement envelope curve, maximum forces, except minor difference due to insufficient modelling of the bond-slip of reinforcing bars and focusing strains in cracked concrete.
2. Moment and load capacity of RC shear wall models have been significantly increased as axial load ratios was increased. These large increases in the capacities of models were taken place at the yielding phase, but load resistances have been dropped at the damage failure to normal levels equal approximately to the resistance of the reference model.
3. Bearing capacities have been improved when thickness to wall height ratios were increased. In this case, the resistance of parametric models had a load – deformation behavior similar to the reference model.
4. Lateral strength capacity of RC shear wall models have been dropped when wall length parameter was reduced. Behavior of load – deformation cures were considerably different from the reference model especially for models that had small values of the wall length.
5. Base section curvatures were decreased as axial load ratios and the wall length increased. Also they had decreased when the thickness to wall lengths ratios increased. Also they had increased as wall lengths and the thickness to wall height ratios increased.
6. New plastic hinge length expression has been proposed here and validated numerically by comparing it with finite- element analysis results taken from other studies. Good agreement and correlation obtained for this predicted equation when compared with other numerically derived expressions.

Then, the proposed equation was verified with data available from experimental studies. It found that there was a clear difference between measured and predicted results because of not including many parameters in the new proposed equation and these parameters had significant effect on calculating the plastic hinge length.

References

[1] Moehle, J. P.: Displacement-Based Design of RC Structures Subjected to Earthquakes. Earthquake Spectra, 8((3)), 403 – 428 (1992)

[2] Dazio, A., Beyer, K., & Bachmann, H.: Quasi-static cyclic tests and plastic hinge analysis of RC structural walls. Engineering Structures, 31(7), 1556-1571 (2009)

[3] Priestly, M.J.N., and Park, R.: Strength and Ductility of Concrete Bridge Columns Under SeismicLoading. ACI Structural Journal, 84((1)), 61 – 76 (1987)

[4] Baker, A. L.: The Ultimate Load Theory Applied to the Design of Reinforced and Prestressed Concrete Frames. (1965)

[5] 428, A.-A. C.: Progress Report on Code Clauses for "Limit Design," 65(9), 713–720 (1986)

[6] Park, R., and Paulay, T. : Reinforced concrete structures, Wiley, New. York. Elwood, K. J., et al. (2007). "Update to ASCE/SEI 41 concrete provisions." Earthq. Spectra, 23(, (3)), 493–523 (1975)

[7] Paulay, T., and Priestley, M. J. N.: Seismic design of reinforced concrete and masonry buildings. Isbn-10 (Vol. 471549150) (1992)

[8] (CEN)., E. C. for S.: Eurocode 8: Design of structures for earthquake resistance: Part 3: Assessment and retrofitting of buildings. BS EN 1998-3, Brussels, Belgium (Vol. 1) (2005)

[9] Panagiotakos, T.B., and Fardis, M. N.: Deformations of Reinforced Concrete Members at Yielding and Ultimate." ACI Structural Journal, 98(2), 135 – 148 (2001)

[10] Biskinis, D., and Fardis, M.: Flexure-controlled ultimate deformations of members with continuous or lap-spliced bars. Structural Concrete, 11(2), 93–108 (2010)

[11] Bohl, A., and Adebar, P.: Plastic hinge lengths in high-rise concrete shear walls. ACI Struct. J., 108((2)), 148–157 (2011)

[12] Ou, Chen, Raditya Andy, N.: Plastic hinge length of reinforced concrete columns. ACI Structural Journal, 105(3), 290–300 (2012)

[13] Kazaz, I.: Analytical Study on Plastic Hinge Length of Structural Walls, (November), 1938–1950 (2013)

[14] Mun, J.: Plastic hinge length of reinforced concrete slender shear walls, 67(8) (2014)

Oesterle, R.G., Aristizabal-Ochoa, J.D., Shiu K.N., and Corley, W. G. (1984). "Web Crushing of Reinforced Concrete Structural Walls." ACI Journal, 81(3), 231 – 241.

[15] Popovics.: A numerical approach to the complete stress-strain curve of concrete. Cement and Concrete Research, 3(5) (1973)

[16] Mander, J., Priestley, M., and Park, R.: Observed Stress-Strain Behavior of Confined Concrete." J. Struct. Eng., 1827, 1827–1849 (1988)

[17] Mander, J. B., Priestley, M. J. N., & R.Park.: Theoretical Stress Strain Model for Confined Concrete. Journal of Structural Engineering (1988)

[18] LUBLINER, Oller, & Barcelona, C.: A plastic-damage model for concrete. International Journal of Solids and Structures, 25(3), 299–326 (1989)

[19] Lee, J. and Fenves, G.: Plastic-Damage Model for Cyclic Loading of Concrete Structures." Journal of Engineering Mechanics, 124(8), 892–900 (1998)

[20] Priestley, M. J. N., Seible, F., and Calvi, G. M.: Seismic design and retrofit of bridges, Wiley, New York (1996)